

# A Two-level GPU-Accelerated Incomplete LU Preconditioner for General Sparse Linear Systems\*

Tianshi Xu <sup>†</sup>

Ruipeng Li <sup>‡</sup>

Daniel Osei-Kuffuor <sup>§</sup>

## Abstract

This paper presents a parallel preconditioning approach based on incomplete LU (ILU) factorizations in the framework of Domain Decomposition (DD) for general sparse linear systems. We focus on distributed memory parallel architectures, specifically, those that are equipped with graphic processing units (GPUs). In addition to block Jacobi, we present general purpose two-level ILU Schur complement-based approaches, where different strategies are presented to solve the coarse-level reduced system. These strategies are combined with modified ILU methods in the construction of the coarse-level operator, in order to effectively remove smooth errors. We leverage available GPU-based sparse matrix kernels to accelerate the setup and the solve phases of the proposed ILU preconditioner. We evaluate the efficiency of the proposed methods as a smoother for algebraic multigrid (AMG) and as a preconditioner for Krylov subspace methods, on challenging anisotropic diffusion problems and a collection of general sparse matrices.

**keywords:** GPU computing; Preconditioning; ILU factorization; Multilevel methods; AMG

## 1 Introduction

This paper considers the problem of solving the linear system

$$Ax = b, \tag{1}$$

where  $A \in \mathbb{R}^{n \times n}$  is large and sparse, which often arises in many fields of science and engineering to compute the numerical solutions of partial differential equations (PDEs). Preconditioned Krylov subspace methods are one class of iterative solvers widely used for solving large sparse systems of linear equations. Here, much of the work has focused on the development of effective preconditioners that can solve the problem at hand in an efficient manner. A general rule of thumb of finding a good preconditioner,  $M$ , is to let  $M \approx A$  such that the eigenvalues of  $M^{-1}A$  are clustered, which can lead to fast convergence of Krylov subspace methods. In addition,  $M$  should be relatively inexpensive to compute and the application of  $M^{-1}$  needs to be performed efficiently. As a result, the iterative solution of the preconditioned system can have better convergence and faster time-to-solution, compared to the iterative solution of the original system (1). We want to emphasize that when considering the efficiency of building and applying preconditioners, one needs to also take into account the underlying computing platforms. The massively parallel processing paradigm on modern many-core processors, like the GPUs considered in this work, have made some traditional preconditioning methods inappropriate on such devices, see e.g., [33, 14].

Algebraic multigrid (AMG) is yet another class of iterative solvers widely used in the linear solver community, both as a stand-alone solver and as a preconditioner. The optimal convergence and scalability of AMG make it an attractive choice for most applications. However, its optimality is restricted to PDEs with elliptic properties.

Incomplete LU (ILU) factorization preconditioners are a class of solvers widely used as general purpose preconditioners for Krylov solvers. Compared with AMG, they are less likely to fail when solving indefinite and ill-conditioned problems or handling irregular meshes. [6, 7, 35, 17, 14]. Extensions and modifications to classical ILU preconditioners, including modified ILU and shifted ILU (with complex shifts) [38, 20, 52, 19, 58, 36], have been proposed for solving indefinite linear systems that arise from applications of Helmholtz equations or interior eigenvalue problems. Such problems are quite difficult to solve by iterative methods since the spectrum of  $A$  includes the origin [15]. Furthermore, ILU methods can also be used as a complex smoother within AMG, thus

---

\*This work was performed under the auspices of the U.S. Department of Energy by Lawrence Livermore National Laboratory under Contract DE-AC52-07NA27344. Work at LLNL was funded by Total S.A. through the FC-MAELSTROM Project.

<sup>†</sup>Department of Computer Science and Engineering, University of Minnesota, Minnesota, USA (xuxx1180@umn.edu)

<sup>‡</sup>Center for Applied Scientific Computing, Lawrence Livermore National Laboratory, California, USA (li50@llnl.gov)

<sup>§</sup>Center for Applied Scientific Computing, Lawrence Livermore National Laboratory, California, USA (oseikuffuor1@llnl.gov)

providing an alternative option for complex problems where standard relaxation-based approaches such as Jacobi and Gauss-Seidel exhibit slow convergence.

While ILU methods can be applied to a wider range of problems, the sequential nature of the algorithm limits its applicability to large scale applications on distributed systems. As a result, there exists active research in the development of efficient parallel ILU strategies. DD-based strategies are some of the most promising strategies. The simplest form of the DD approach is the block Jacobi ILU approach, where only the local block corresponding to individual subdomains are factorized, ignoring any inter-domain coupling. In [37], the authors proposed a DD-based global Schwarz preconditioning, where the ILU is used as a complex smoother for local geometric multigrid, and GPU is used to accelerate the triangular solve. A more accurate alternative is the so-called two-level ILU strategy, where a local factorization is first performed within each subdomain, followed by a global strategy to account for the inter-domain coupling. Common approaches for the global strategy include a graph-based global ILU factorization of the coupling matrix (Schur complement) [29, 26]; and standard algebraic Schur complement strategies [50, 13]. Partial ILU techniques or incomplete triangular solves may be used to control the sparsity of the Schur complement in the latter approach [44]. The work presented in this paper utilizes the standard algebraic Schur complement strategies with partial ILU techniques. In [13], a two-level ILU preconditioner is developed specifically for electromagnetic applications. There, the global Schur complement is assembled on a single node and factorized sequentially. While the authors mention its suitability on distributed systems, the algorithm is evaluated on a single node using shared-memory parallelism. Perhaps, the most relevant works in the literature related to the approach proposed in this paper are [50] and [44]. In [50], Saad and Zhang proposed a parallel multilevel threshold-based ILU preconditioning technique based on DD. A partial ILU strategy is used to construct the Schur complement, which may be further reduced to multiple levels. The last level matrix is then assembled on a single node and factorized. In [44], the authors propose a two-level level-based ILU preconditioner that also utilizes partial ILU to construct the Schur complement corresponding to the global coupling. Here, they form a local Schur complement on each subdomain following [11], and solve them locally to approximately solve the global Schur complement system. Both of these methods, while applicable to distributed systems, do not utilize potential enhancements offered by GPUs. It is worth mentioning that the notion of global Schur complement updates in the context of DD is also applicable to parallel sparse direct solvers [51].

Since the advent of CUDA, the NVIDIA GPUs have gained a lot of attention for accelerating sparse linear solvers [41, 47, 51, 57, 16, 48, 22, 8, 33, 49] and eigensolvers [3, 18, 4, 34], the performance gains of which are usually from the accelerated sparse matrix computation kernels. GPUs have also been used to accelerate parallel ILU factorizations. Packages such as PARALUTION [31] and HIFLOW [23] provide distributed memory ILU factorizations with GPU support. However, the implementation in these packages follow a block-Jacobi approach.

In this paper, we present a DD-based two-level parallel ILU strategy designed for distributed memory systems and with GPU support. We summarize below the main contributions of this paper.

- We provide a detailed analysis of the two-level strategy, showing the benefit of using modified ILU to achieve faster convergence.
- The algorithm supports several parallel ILU strategies, including the standard block Jacobi approach; a two-level additive ILU approach, where the coarse grid is obtained implicitly via a partial ILU factorization; and a two-level multiplicative ILU approach, where the coarse grid system is obtained via a Galerkin product akin to AMG methods.
- This work is implemented within the hypre [21] package, making it readily available to application developers. The implementation is MPI-based, which supports distributed memory systems, and the ILU preconditioners proposed in this paper take advantage of the existing accelerated kernels for computing the ILU(0) factorization and solving sparse triangular linear systems on GPUs.

The remainder of this paper is organized as follows: in Section 2 we review the DD framework and present several parallel preconditioning algorithms of ILU factorizations based on DD. We then present the parallel implementation details of these algorithms with respect to GPUs in Section 3. In Section 4, we present numerical results on our evaluation of the performance of the different preconditioning strategies, and we conclude in Section 5.

## 2 Parallel ILU via domain decomposition

DD methods are widely used for solving coupled systems of PDEs over physical domains with different properties, particularly in the context of parallel computing. The most general and versatile approach of DD, which is also purely algebraic, often resorts to partitioning the underlying graph of the matrix with graph partitioners [12, 25, 28, 30, 45, 46]. Here we assume that the global system has been partitioned into  $p$  subdomains, each assigned a set of equations, which is stored locally. Then, corresponding to this partitioning, the global system (1)

can be written as

$$\begin{pmatrix} A_1 & E_{12} & \cdots & E_{1p} \\ E_{21} & A_2 & \cdots & E_{2p} \\ \vdots & \vdots & \ddots & \vdots \\ E_{p1} & E_{p2} & \cdots & A_p \end{pmatrix} \begin{pmatrix} x_1 \\ x_2 \\ \vdots \\ x_p \end{pmatrix} = \begin{pmatrix} b_1 \\ b_2 \\ \vdots \\ b_p \end{pmatrix}, \quad (2)$$

where the local system for subdomain  $i$  reads

$$A_i x_i + \sum_{j \in \mathcal{N}_i} E_{ij} x_j = b_i, \quad (3)$$

where  $A_i$  is the operator that acts on the local degrees of freedom  $x_i$ ,  $\mathcal{N}_i$  is a set of the indices of the subdomains that are adjacent to  $i$ , and  $E_{ij}$  represents the connections between subdomains  $i$  and  $j$ .

## 2.1 One-level block Jacobi approach

One of the simplest ways to precondition (2) in parallel would be to use the block Jacobi approach. In this approach, (2) is approximately solved by ignoring all the off-diagonal coupling in the coefficient matrix. For each subdomain, the local system  $A_i x_i = b_i$  is solved instead, dropping the coupling terms  $E_{ij} x_j$  in (3). Furthermore, the local systems are often approximately solved by methods such as the ILU factorizations. This approach is simple and requires no communication in building and applying the preconditioner. However, a common issue with this approach is that the convergence of Krylov subspace methods combined with it generally deteriorates as the number of subdomains increases and as the size of the system grows. In addition, ignoring off-diagonal terms limits the effectiveness of this block Jacobi strategy to systems with weak off-diagonal coupling. The convergence could be improved using restricted additive Schwarz method [10], but the memory cost is slightly higher. We note that although this block Jacobi strategy is not scalable (for the reasons mentioned above), it can be incorporated into AMG as an alternative to the standard smoothers when solving complex problems.

## 2.2 Two-level block ILU approach

### 2.2.1 Domain decomposition and local partitioning

To reduce the sensitivity of the preconditioner to the number of subdomains, the two-level approach further takes advantage of the DD framework by first partitioning and reordering the nodes of the local subdomain into interior and exterior nodes. Fig. 1 shows a DD of a 2-D grid into 4 subdomains. The interior nodes in each subdomain connect only to other nodes inside the subdomain. These are identified by the (unfilled) circles in Fig. 1. In contrast, the exterior nodes, black dots in Fig. 1, can have connections to nodes from other subdomains. These connections are shown by the solid black lines. If we re-label the unknowns such that all the interior nodes are labeled first, followed by the exterior nodes, the global coefficient matrix can be reordered as shown in the right graph of Fig. 1, where the upper left part of the matrix is now block diagonal, and each diagonal block corresponds to a subdomain.

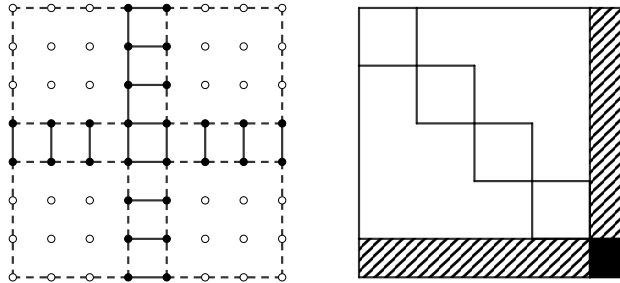


Figure 1: DD of mesh points (left) and the corresponding reordered global coefficient matrix (right).

From the point of view of the system of equations, the reordered system  $Ax = b$ , corresponding to the DD can be written as

$$\begin{pmatrix} B & F \\ E & C \end{pmatrix} \begin{pmatrix} u \\ v \end{pmatrix} = \begin{pmatrix} f \\ g \end{pmatrix}, \quad (4)$$

---

**Algorithm 1** Additive block ILU solve

---

- 1: Compute  $\hat{g} = g - EB^{-1}f$
  - 2: Solve  $v = S^{-1}\hat{g}$  with  $S = C - EB^{-1}F$
  - 3: Solve  $u = B^{-1}(f - Fv)$
- 

where  $B \in \mathbb{R}^{n_1 \times n_1}$  is block diagonal associated with the interior nodes,  $C \in \mathbb{R}^{n_2 \times n_2}$  corresponds to the exterior nodes, and  $E$  and  $F$  contain the local couplings. We can write the block LDU factorization of  $A$  of the form:

$$\begin{pmatrix} I & \\ EB^{-1} & I \end{pmatrix} \begin{pmatrix} B & \\ & S \end{pmatrix} \begin{pmatrix} I & B^{-1}F \\ & I \end{pmatrix} \begin{pmatrix} u \\ v \end{pmatrix} = \begin{pmatrix} f \\ g \end{pmatrix}, \quad (5)$$

where  $S = C - EB^{-1}F$  is the global Schur complement matrix. It is easy to verify that the inverse of the block LDU factorization of  $A$  is given by

$$A^{-1} = \begin{pmatrix} I & -B^{-1}F \\ & I \end{pmatrix} \begin{pmatrix} B^{-1} & \\ & S^{-1} \end{pmatrix} \begin{pmatrix} I & \\ -EB^{-1} & I \end{pmatrix}. \quad (6)$$

### 2.2.2 Reduced system with the global Schur complement

The typical approach of solving (4) is to first solve for the interface unknowns  $v$  from the reduced system with the Schur complement, which is then substituted back into (4) to obtain the solution for interior unknowns  $u$ . Note here that, due to the block structure from DD, the solves with  $B$  and the multiplications with  $E$  and  $F$  can be done locally without communicating with other processors. The only part that requires communication is in solution of the Schur complement system. Moreover, the global Schur complement matrix  $S = C - EB^{-1}F$  can be constructed efficiently in parallel. The local computations  $S_i = C_i - E_i B_i^{-1} F_i$ , yield the diagonal blocks of  $S$ , and the remaining entries of  $S$  are the same as the entries in the off-diagonal blocks of the submatrix  $C$  of the original coefficient matrix. Thus, it is easy to see that this approach is amenable to parallel computing. By and large, having a smaller Schur complement usually leads to better parallel performance.

To construct a preconditioner using this framework,  $B$  is approximated by its ILU factorization,  $B \approx LU$ , and the Schur system  $Sy = \hat{g}$  is only solved approximately. The two-level block ILU approach is summarized in Algorithm 1, where  $B^{\sim 1}$  and  $S^{\sim 1}$  denote that the actions of  $B^{-1}$  and  $S^{-1}$  are approximately applied. It is easy to see that the parallel efficiency of the preconditioning technique in Algorithm 1 depends on the strategy used to solve the global Schur complement system. One strategy for performing this solve with  $S$  is to use a small number of GMRES iterations preconditioned with the block Jacobi preconditioner that consists of the local Schur complements  $S_i$ . The inverse of the local Schur complements can be applied using their ILU factorizations. Note that this factorization can be obtained by factorizing the local  $B$  matrix. Two different implementations of this approach for solving the global Schur complement system will be discussed in detail in Section 3.2.

### 2.2.3 Galerkin product and coarse-grid correction

Another way to view the aforementioned block ILU methods is from the perspective of coarse correction as in the AMG methods. We can rewrite (6) as

$$A^{-1} = \begin{pmatrix} G & P^* \\ & S^{-1} \end{pmatrix} \begin{pmatrix} B^{-1} \\ & R^* \end{pmatrix}, \quad (7)$$

where  $G = (I, 0)^T$ ,  $P^*$  and  $R^*$  are the so-called ideal interpolation and restriction operators, given by

$$P^* = \begin{pmatrix} -B^{-1}F \\ I \end{pmatrix}, \quad R^* = \begin{pmatrix} -EB^{-1} & I \end{pmatrix}, \quad (8)$$

respectively. It is easy to verify that the coarse-grid operator computed by the Galerkin product with  $P^*$  and  $R^*$  is the Schur complement, i.e.,  $R^*AP^* = S$ , and the exact solution can be obtained by

$$x = (GB^{-1}G^T + P^*S^{-1}R^*)b. \quad (9)$$

In the context of preconditioning, practical interpolation and the restriction operators are usually constructed as sparser approximations to the ideal ones, which in this work are assumed to have the form of

$$P = \begin{pmatrix} -B^{\sim 1}F \\ I \end{pmatrix} \quad \text{and} \quad R = \begin{pmatrix} -EB^{\sim 1} & I \end{pmatrix}. \quad (10)$$

Proposition 1 describes the energy-norm minimization property of  $P^*$  and its connection with a general  $P$ . In what follows, we denote the range of an operator  $H$  as  $\text{Ran}(H)$ .

---

**Algorithm 2** Two-level multiplicative solve
 

---

- |   |                 |
|---|-----------------|
| 1: Compute $\hat{x} = GB^{\sim 1}G^T b$   | ▷ F-relaxation  |
| 2: Compute $r = R(b - A\hat{x})$          | ▷ Restriction   |
| 3: Solve $v = S^{\sim 1}r$ with $S = RAP$ | ▷ C-correction  |
| 4: Compute $x = \hat{x} + Pv$             | ▷ Interpolation |
- 

**Proposition 1.** For an SPD matrix  $A$ , the ideal interpolation  $P^*$  is the  $A$ -orthogonal projection of any  $P$  of the form  $P^T = (W^T, I)$  onto subspace  $\text{Range}(G)^{\perp A}$ , where  $G = (I, 0)^T$ . Moreover,  $\|P\|_A \geq \|P^*\|_A, \forall P$ .

*Proof.* Let  $Q_A = GB^{-1}G^T A$ , which is an  $A$ -orthogonal projector. It is easy to verify that  $(I - Q_A)P = P^*$ . For the second part,  $\|Pv\|_A^2 = \|P^*v\|_A^2 + \|(I - Q_A)Pv\|_A^2 \geq \|P^*v\|_A^2$ , so  $\|Pv\|_A \geq \|P^*v\|_A$  and the result follows.  $\square$

Similar property can be also shown for  $(R^*)^T$ . Given  $P$  and  $R$  in (10), Algorithm 2 presents this two-level preconditioning approach.

**Remark 1** (Comparison between Algorithm 1 and Algorithm 2).

1. The solution from Algorithm 1 can be reformulated as (9) with  $P$  and  $R$  defined in (10), where the relaxation  $GB^{\sim 1}G^T$  and the coarse-grid correction  $PS^{\sim 1}R$  are additively [27] applied to  $b$ .
2. The solution  $x$  from Algorithm 2 can be expressed as

$$x = (GB^{\sim 1}G^T + PS^{\sim 1}R(I - AGB^{\sim 1}G^T))b,$$

which is multiplicative [53] and equivalent to the additive form (9) when  $R = R^*$ , since  $R^*AG = 0$ .

3. The Schur complement in Algorithm 1 denoted by  $S_{A_1} = C - EB^{-1}F$  is equal to  $R_0AP$  with  $R_0 = (0, I)$ . Comparing with the Schur complement in Algorithms 2, denoted by  $S_{A_2} = RAP$ , we have  $S_{A_2} - S_{A_1} = EB^{\sim 1}BB^{\sim 1}F - EB^{-1}F$ .
4. When  $B^{\sim 1}$  is sufficiently accurate, the preconditioning qualities of Algorithms 1 and 2 are generally similar, whereas for less accurate  $B^{\sim 1}$ , the multiplicative approach in Algorithm 2 is often better. On the other hand,  $S_{A_2}$  is generally denser than  $S_{A_1}$  and more expensive to build.

In this work, we consider an ILU(0) factorization for  $B^{\sim 1}$  in order to benefit from optimized kernels that efficiently perform the factorization as well as forward and backward solves on GPUs. Using ILU(0), we found that the approach in Algorithm 2, in general, has much faster convergence and better overall performance.

### 2.3 Modified ILU factorizations for building $P$

It is clear that the interpolation matrix  $P$  of the form in (10) solely depends on the choice of  $B^{\sim 1} = U^{-1}L^{-1}$ . In this section, we will show constructing  $P$  from a modified ILU(0) factorization of  $B$  yields a better interpolation operator, compared to using standard ILU(0). To show this, it is useful to examine the error propagation of Algorithm 2, which can be written as

$$e_{i+1} := (I - P(RAP)^{\sim 1}RA)(I - GB^{\sim 1}G^T A)e_i, \quad (11)$$

where  $e_i$  denotes the error in the solution at iteration  $i$ . Suppose  $(RAP)^{\sim 1}$  is exact, and then  $I - P(RAP)^{\sim 1}RA$  is an  $A$ -orthogonal projector that has the range of  $P$ , denoted by  $\text{Ran}(P)$ , as its kernel. Therefore, to reduce the “smooth” errors that cannot be effectively removed by the smoothing step  $I - GB^{\sim 1}G^T A$  in (11), it is important to include the smooth errors in  $\text{Ran}(P)$ . For elliptic-type PDEs, constant vectors represent the smoothest mode of  $A$ . As a result, standard AMG algorithms typically use interpolation formulae that can interpolate constant vectors exactly.

Using ILU, we show that the interpolation operator  $P$  can also be constructed to have a chosen vector in its range. Specifically, in order to have a given vector

$$\begin{pmatrix} y \\ z \end{pmatrix} \in \text{Ran}(P), \quad \text{where} \quad P = \begin{pmatrix} -U^{-1}L^{-1}F \\ I \end{pmatrix}, \quad (12)$$

we need to let

$$-U^{-1}L^{-1}Fz = y \quad \text{or} \quad LUy = -Fz. \quad (13)$$

The ILU factorization of  $B$  can be written as

$$B = LU + H, \quad (14)$$

where  $H$  contains the elements that are dropped entries during the process of the factorization, so (13) is equivalent to

$$(B - H)y = -Fz \quad \Leftrightarrow \quad Hy = By + Fz \equiv w, \quad (15)$$

which can be satisfied by compensating the diagonal of  $U$ . Consider the  $i$ -th step of a row-wise ILU factorization,

$$H_{i,:} = B_{i,:} - \sum_{j \leq i} l_{ij} U_{j,:}, \quad l_{ii} = 1, \quad (16)$$

where  $H_{i,:}$ ,  $B_{i,:}$  and  $U_{j,:}$  denote the  $i$ -th and the  $j$ -th row of  $H$ ,  $B$  and  $U$  respectively. In general, we do not explicitly have  $H_{i,:}y = w_i$ . However, it can be enforced by adding some perturbation to  $u_{ii}$  to get  $u_{ii} + \Delta_i$ . Correspondingly,  $H_{i,:}$  becomes  $H_{i,:} - \Delta_i e_i^T$ , where  $e_i$  is the  $i$ -th column of the identity matrix. Substituting this perturbed  $H_{i,:}$  into (15), we obtain

$$\Delta_i = \frac{H_{i,:}y - w_i}{y_i}. \quad (17)$$

For elliptic PDE operators, the vectors of interest  $y$  and  $z$  are constant vectors, and furthermore,  $By + Fz = 0$ . Thus,  $\Delta_i$  in (17) reduces to  $\Delta_i = \sum_j H_{i,j}$ , i.e., the sum of the dropped entries during the factorization of row  $i$ , which is the standard modified ILU (MILU) algorithm[39].

In this work, the MILU(0) factorization is used to compute the interpolation and restriction operators, while a different factorization such as standard ILU(0) can be used in the smoothing step.

### 3 Parallel implementation details

In this section, we discuss the implementation details of the ILU-based preconditioners mentioned in the previous sections on both CPUs and GPUs.

#### 3.1 Block Jacobi preconditioner with ILU

The implementation of the block Jacobi ILU is rather straightforward. During the setup phase, we apply an ILU factorization to each local diagonal block  $A_i$  after re-labeling and ordering the local subdomain into interior and exterior nodes, as discussed previously. Fill-reducing reordering may be used to improve the accuracy and stability of the ILU factorization. In this work, we use the RCM strategy [24] to reorder the local diagonal matrix  $A_i$  prior to the ILU factorization.

For the GPU implementation, we use the state-of-the-art ILU(0) routine from the Nvidia cuSPARSE library, which is based on the level-scheduling algorithm [33, 43]. An analysis routine is required before the actual numerical factorization, which generates the level information in order to exploit the parallelism in the factorization. After that, the rows in the same level can be factorized at the same time to utilize the many-core architecture of GPUs. This level-scheduling algorithm normally works well for many applications, especially in the cases where the number of levels is not too large. In the solve phase, we also take advantage of the sparse triangular solve routine from the cuSPARSE library. This routine also utilizes level-scheduling, so that the unknowns in the same level can be solved simultaneously.

One of the major differences between the CPU and the GPU implementations of the proposed preconditioners is the requirement of explicit reordering of the unknowns to match their label as interior or exterior nodes. In the CPU implementation, an explicit reordering of the matrix can be avoided, and the factorization and subsequent triangular solves can be performed implicitly with a permutation array. However, the cuSPARSE library does not support the use of permutation arrays, so the matrix has to be explicitly permuted before calling the factorization routine. As a result, a copy of the matrix with the new ordering has to be saved. However, since the computed factors are stored in the same memory of the input matrix (without the unit diagonal of the  $L$ -factor), storing the extra permuted matrix actually does not require more memory compared with the CPU implementation, where the  $L$  and  $U$  factors are stored in different matrices. Furthermore, switching between the  $L$  and the  $U$  factors in the triangular solves can be done by using the matrix descriptor of cuSPARSE, which removes the need of storing the two triangular matrices separately. The setup and the solve phases of the block Jacobi ILU preconditioner on GPUs are summarized in Algorithm 3, where the `gather` and the `scatter` functions from `thrust` are used for permuting the input and the output vectors of the solve.

#### 3.2 Computing the global Schur complement and two-level additive solve

In this section, we discuss the details of the two-level ILU preconditioner based on Algorithm 1. Recall that the Schur complement from the DD is defined as  $S = C - EB^{-1}F$ . Let  $A_i$  denote the submatrix defined

---

**Algorithm 3** Block Jacobi ILU on GPU

---

1: **procedure** BJILU-SETUP( $A$ ) ▷ Distributed CSR matrix  
2:   Compute the RCM ordering  $p_i$  of  $A_i$   
3:   Reorder  $A_i$  to  $A_i^{p_i}$  with  $p_i$   
4:   Call cuSPARSE to compute ILU(0) of  $A_i^{p_i}$   
5:   Setup triangular solve  
6: **end procedure**  
7: **procedure**  $x =$  BJILU-SOLVE( $b$ )  
8:   Call `thrust::gather` on  $b_i$  with permutation  $p_i$   
9:   Call cuSPARSE to solve  $L_{A_i}U_{A_i}x_i = b_i$   
10:   Call `thrust::scatter`  $x_i$  with permutation  $p_i$   
11: **end procedure**

---

on subdomain  $i$ , from the DD. Suppose that the unknowns are locally ordered as interior and exterior nodes as previously discussed, then  $A_i$  can be written as: Assume that the local submatrix  $A_i$  (corresponding to subdomain  $i$ ) takes the form

$$A_i = \begin{pmatrix} B_i & F_i \\ E_i & C_i \end{pmatrix}. \quad (18)$$

An important result from the DD in (4) is that  $B$  is block diagonal with  $B_i$  on the diagonal. The same is true for  $E$  with  $E_i$  and  $F$  with  $F_i$ . Thus, the term  $EB^{-1}F$  from  $S$  is also block diagonal. Furthermore, the diagonal blocks of  $S$ , denoted by  $S_i$ , can be computed locally as  $S_i = E_iB_i^{-1}F_i$ . The off-diagonal blocks of  $S$  are the same as in  $C$ , denoted by  $E_{ij}$ , which couples the domains  $i$  and  $j$ . Therefore, the reduced Schur complement system  $Sy = g'$  takes the following form,

$$\begin{pmatrix} S_1 & E_{12} & \cdots & E_{1p} \\ E_{21} & S_2 & \cdots & E_{2p} \\ \vdots & \vdots & \ddots & \vdots \\ E_{p1} & E_{p2} & \cdots & S_p \end{pmatrix} \begin{pmatrix} y_1 \\ y_2 \\ \vdots \\ y_p \end{pmatrix} = \begin{pmatrix} g'_1 \\ g'_2 \\ \vdots \\ g'_p \end{pmatrix}. \quad (19)$$

In practice, computing the exact  $S_i$  is usually too expensive and an approximation is preferred instead. Approximations to  $S_i$ , denoted by  $\tilde{S}_i$ , obtained by dropping small entries, can be used in the place of  $S_i$ . Forming the local matrices  $\tilde{S}_i$  and thus having the explicit form of a matrix that approximates the global Schur complement provides the flexibility of choosing different methods to solve the reduced system (19). Two approaches for computing  $\tilde{S}_i$  have been considered. In the first approach we compute  $\tilde{S}_i = C_i - E_iU_{B_i}^{-1}L_{B_i}^{-1}F_i$  with the ILU factorization of  $B_i$ , where  $L_{B_i}$  and  $U_{B_i}$  denote the computed  $L$  and  $U$  factors of  $B_i$ . For the term  $E_iU_{B_i}^{-1}L_{B_i}^{-1}F_i$ , we first compute the two intermediate matrices  $W_i = E_iU_{B_i}^{-1}$  and  $Z_i = L_{B_i}^{-1}F_i$ , and then compute  $S_i = C_i - W_iZ_i$ . Note that in the above computations, the sparse triangular solves to compute  $W_i$  and  $Z_i$  should be done carefully to exploit the sparsity. Furthermore, sparse matrix-matrix multiplications is needed for  $W_iZ_i$ . In practice it is often necessary to drop small entries in order to keep the cost of these computations inexpensive and the resulting approximation  $\tilde{S}_i$  sparse.

An alternative approach to compute  $\tilde{S}_i$  that is more flexible and potentially more efficient, is to use the idea of partial ILU factorization. In this approach, the ILU factorization of  $A_i$  skips the elimination steps within the (2, 2) block corresponding to the Schur complement. To be succinct, the ILU factorization of  $A_i$  can be written as

$$\begin{pmatrix} L_{B_i} & \\ E_iU_{B_i}^{-1} & L_{S_i} \end{pmatrix} \begin{pmatrix} U_{B_i} & L_{B_i}^{-1}F_i \\ & U_{S_i} \end{pmatrix}, \quad (20)$$

whereas, the partial ILU factorization, can be written as

$$\begin{pmatrix} L_{B_i} & \\ E_iU_{B_i}^{-1} & I \end{pmatrix} \begin{pmatrix} U_{B_i} & L_{B_i}^{-1}F_i \\ & \tilde{S}_i \end{pmatrix}. \quad (21)$$

Note that the difference between the two factorizations is in the (2, 2) block, where the desired Schur complement appears in the corresponding block of the  $U$  matrix. Figure 2 provides an illustration of the partial ILU and the full ILU factorizations.

Compared to the previous approach for computing  $\tilde{S}_i$ , there exist several advantages on the flexibility and the efficiency in the partial ILU factorization approach:

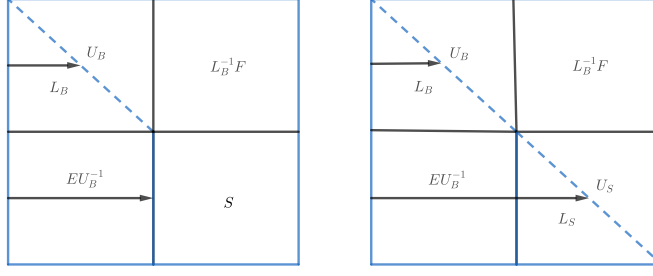


Figure 2: Illustration of the partial ILU factorization, which leaves an approximation to the Schur complement at the (2,2) block (left), and the normal ILU factorization, which computes an ILU factorization of the Schur complement as well (right)

1. Different dropping criteria can be applied in the different blocks of  $A_i$ , which provides full flexibility of controlling the accuracy and the sparsity of the resulting matrices  $L_{B_i}$ ,  $U_{B_i}$ ,  $E_i U_{B_i}^{-1}$ ,  $L_{B_i}^{-1} F_i$  and  $\tilde{S}_i$ .
2. Matrices  $W_i = E_i U_{B_i}^{-1}$ ,  $Z_i = L_{B_i}^{-1} F_i$  and  $\tilde{S}_i$  can be implicitly computed in a partial ILU factorization all at once, which is typically more efficient than computing them separately as in the pervious approach.

In the CPU implementation, we adopt the latter approach of using the partial ILU factorization to compute  $\tilde{S}_i$ . In Algorithm 1, two solves with  $B_i$  are required by applying  $U_B^{-1} L_B^{-1}$ . On the other hand, if the intermediate matrices that approximate  $W = E U_B^{-1}$  and  $Z = L_B^{-1} F$  from the partial ILU factorization are stored as well, then the two-level solve can be performed with only one solve with  $L_{B_i}$  and  $U_{B_i}$ , as follows:

- 
- 1: Local solve  $f'_i = L_{B_i}^{-1} f_i$
  - 2: Compute  $g'_i = g_i - W_i f'_i$
  - 3: Global solve  $S y = g'$
  - 4: Local solve  $u_i = U_{B_i}^{-1} (f'_i - Z_i y_i)$
- 

For the GPU implementation, there are several technical difficulties for using the afore mentioned strategies to compute  $\tilde{S}_i$  explicitly. First, there is no available routine to compute the partial ILU(0) factorization on GPUs; Second, efficient implementation of sparse triangular solves with multiple sparse right-hand sides and sparse matrix-matrix multiplications, needed to compute  $\tilde{S}_i = C_i - (E_i U_{B_i}^{-1}) (L_{B_i}^{-1} F_i)$ , can be challenging on GPUs. The strategy adopted for the GPU implementation follows from reformulating the system in (19) by preconditioning with a diagonal (block Jacobi) preconditioner. The resulting linear system has the following form:

$$\begin{pmatrix} I & \tilde{S}_1^{-1} E_{12} & \cdots & \tilde{S}_1^{-1} E_{1p} \\ \tilde{S}_2^{-1} E_{21} & I & \cdots & \tilde{S}_2^{-1} E_{2p} \\ \vdots & \vdots & \ddots & \vdots \\ \tilde{S}_p^{-1} E_{p1} & \tilde{S}_p^{-1} E_{p2} & \cdots & I \end{pmatrix} \begin{pmatrix} y_1 \\ y_2 \\ \vdots \\ y_p \end{pmatrix} = \begin{pmatrix} \tilde{S}_1^{-1} g'_1 \\ \tilde{S}_2^{-1} g'_2 \\ \vdots \\ \tilde{S}_p^{-1} g'_p \end{pmatrix}. \quad (22)$$

Notice that the explicit form of  $\tilde{S}_i$  is not needed and only the application of  $\tilde{S}_i^{-1}$  is required.  $\tilde{S}_i^{-1}$  is approximated by  $U_{S_i}^{-1} L_{S_i}^{-1}$ , where  $L_{S_i}$  and  $U_{S_i}$  are the submatrices corresponding to the Schur complement block of the ILU(0) factors of  $A_i$ . We remark that  $L_{S_i} U_{S_i}$  is not the ILU(0) factorization of the Schur complement, since the sparsity patterns of  $L_{S_i}$  and  $U_{S_i}$  match that of  $C_i$ . In our implementation, we compute the ILU(0) factorization of  $A_i$  and then extract the factors of  $L_{B_i}$ ,  $U_{B_i}$ ,  $L_{S_i}$  and  $U_{S_i}$ . Krylov subspace iterations are applied to (22), which only requires the coefficient matrix in the form of MATVEC. The solution is achieved by performing:

$$y_i + \tilde{S}_i^{-1} \sum_{j \in \mathcal{N}_i} \hat{E}_{ij} y_j, \quad (23)$$

within each subdomain, where a MATVEC with the off-diagonal matrix of  $A$  is needed, followed by triangular solves with  $L_{S_i}$  and  $U_{S_i}$ . Therefore, the communication cost of the MATVEC with the coefficient matrix in (22) is exactly the same as that with the original matrix  $A$ . The implementation of the two-level ILU solve on GPUs is presented in Algorithm 4.



---

**Algorithm 4** Additive SCHUR-ILU on GPU

---

```
1: procedure SCHUR-ILU SETUP( $A$ ) ▷ Distributed CSR matrix
2:   Compute local permutation  $p_i$ 
3:   Permute  $A_i$  to  $A^{p_i}$  with  $p_i$ 
4:   Call cuSPARSE to compute ILU(0) of  $A^{p_i}$ 
5:   Extract factors  $L_{B_i}, U_{B_i}, L_{S_i}, U_{S_i}, E_i U_{B_i}^{-1}$ , and  $L_{B_i}^{-1} F_i$ 
6:   Setup triangular solve
7:   return  $L_{B_i}, U_{B_i}, L_{S_i}, U_{S_i}, E_i U_{B_i}^{-1}$ , and  $L_{B_i}^{-1} F_i$ 
8: end procedure
9: procedure SCHUR-ILU SOLVE( $b$ ) ▷ Solve for  $x$  with right-hand-side  $b$ 
10:  Call thrust::gather to permute  $b_i$  with  $p_i$ 
11:  Call cuSPARSE to solve for  $f'_i = L_{B_i}^{-1} f_i$ 
12:  Compute  $g'_i = g_i - E_i U_{B_i}^{-1} f'_i$ 
13:  Apply GMRES to (22) to solve for  $y$ 
14:  Compute  $f''_i = f'_i - L_{B_i}^{-1} F_i y_i$ 
15:  Call cuSPARSE to solve  $u_i = U_{B_i}^{-1} f''_i$ 
16:  Call thrust::scatter to permute  $x_i$  with  $p_i$ 
17:  return  $x$ 
18: end procedure
```

---

### 3.3 Two-level multiplicative solve

In this section, we discuss the implementation of the two-level multiplicative approach corresponding to Algorithm 2. MILU(0) factorization was used to construct  $R$  and  $P$ , while standard ILU(0) is used as the smoother. Thus, two different ILU(0) factorizations were required, which doubles the memory cost. Nonetheless, this combination often yielded better overall convergence compared to using MILU(0) as the smoother. From (10) and subsequent discussions herein, it is easy to see that computing the exact  $R$  and  $P$  and the subsequent  $RAP$  product is impractical. Moreover, explicitly forming these matrices is particularly difficult on GPUs as mentioned before. Therefore, in this approach,  $R$ ,  $P$  and  $RAP$  are unformed. Instead, only  $L_B$  and  $U_B$  are stored, since the matrix  $RAP$  is needed only in the form of the MATVEC to apply Krylov subspace methods on reduced Schur complement system. With this unformed  $RAP$ , the MATVEC requires four local triangular solves with  $L_{B_i}$  and  $U_{B_i}$ , two for applying  $P$  and two for multiplying  $R$  respectively. One way to reduce the cost of these evaluations is to use approximations of  $W \equiv EU_B^{-1}$  and  $Z \equiv L_B^{-1}F$  that is available from the ILU factorization of  $A$ , which can reduce the number of the triangular solves required in the MATVEC with  $RAP$  by a factor of two. Assume that the ILU factors of  $A$  are

$$L = \begin{pmatrix} L_B & \\ \tilde{W} & L_S \end{pmatrix} \quad \text{and} \quad U = \begin{pmatrix} U_B & \tilde{Z} \\ & U_S \end{pmatrix}, \quad (24)$$

where  $\tilde{W}$  and  $\tilde{Z}$  approximate  $W$  and  $Z$  respectively. Then, it follows that the  $P$  and  $R$  in (10) can be given by

$$P = \begin{pmatrix} -U_B^{-1} \tilde{Z} \\ I \end{pmatrix} \quad \text{and} \quad R = \begin{pmatrix} -\tilde{W} L_B^{-1} & I \end{pmatrix}, \quad (25)$$

where  $-U_B^{-1} \tilde{Z}$  and  $-\tilde{W} L_B^{-1}$  are kept unformed. As a result, only two solves with  $L_B$  and  $U_B$  are needed to perform the MATVEC with  $RAP$ . In Section 2.3, we showed how MILU(0) of  $B$  can be used to construct  $P$  in (12). Similarly, MILU(0) of  $A$  can also be utilized here to ensure that a given vector is in  $\text{Ran}(P)$ . To see this, suppose the ILU factorization  $A = LU + H$  has the following 2-by-2 block form,

$$\begin{pmatrix} B & F \\ E & C \end{pmatrix} = \begin{pmatrix} L_B U_B + H_{11} & L_B \tilde{Z} + H_{12} \\ \tilde{W} U_B + H_{21} & \tilde{W} \tilde{Z} + L_S U_S + H_{22} \end{pmatrix}. \quad (26)$$

Having vector  $\begin{pmatrix} y \\ z \end{pmatrix} \in \text{Ran}(P)$  leads to the following equation,

$$Pz = \begin{pmatrix} -U_B^{-1} \tilde{Z} \\ I \end{pmatrix} z = \begin{pmatrix} y \\ z \end{pmatrix}, \quad (27)$$

and thus

$$U_B y = -\tilde{Z} z \Rightarrow L_B U_B y = -L_B \tilde{Z} z, \quad (28)$$

together with (26), we have

$$(B - H_{11}) y = (H_{12} - F) z, \quad (29)$$

which can be rewritten as

$$H_{11} y + H_{12} z = B y + F z \equiv w \quad (30)$$

which leads to the MILU of  $A$ .

From (27), the corresponding  $RAP$  is now

$$RAP = \begin{pmatrix} -\tilde{W} L_B^{-1} & I \end{pmatrix} \begin{pmatrix} B & F \\ E & C \end{pmatrix} \begin{pmatrix} -U_B^{-1} \tilde{Z} \\ I \end{pmatrix}. \quad (31)$$

The remaining task is to build a preconditioner for the coarse-grid operator  $RAP$ , so that we can effectively apply Krylov subspace methods to solve the coarse-grid problem. Expanding the expression of  $RAP$  in (31) and using (26),  $RAP$  can be expressed as

$$RAP = L_S U_S + RHP. \quad (32)$$

The residual matrix  $H$  contains the dropped elements during the ILU factorization. These elements decrease in size as the accuracy of the factorization increases, and when the factorization is exact,  $H$  is zero. Thus, it makes sense to use  $L_S U_S$  as the preconditioner of  $RAP$ . Moreover, if  $L_S$  and  $U_S$  are obtained from the MILU(0) factorization of  $A$  as described above, the preconditioner can also preserve the action on the constant vector. That is,

$$RAP \mathbf{1} = L_S U_S \mathbf{1}, \quad (33)$$

where  $\mathbf{1}$  denotes the vector of all ones, which can be easily shown from  $P \mathbf{1} = \mathbf{1}$  and  $H \mathbf{1} = 0$ . This property is known to be important for preconditioning elliptic operators [39].

In our implementation, we compute the MILU(0) factorization of each  $A_i$ , and extract the factorization of  $B_i$  from the (1,1) blocks of the factors, while the  $\tilde{W}_i$  and  $\tilde{Z}_i$  matrices are available in the corresponding (2,1) and (1,2) blocks. The remaining (2,2) blocks, which are the ILU factorization of  $S_i$ , is used as the preconditioner for  $S_i$ . A technical problem for the GPU implementation of this approach is that there is currently no available routine for MILU(0) on GPUs. For this reason, we simply leave the computation of the MILU(0) factorization on CPU for now. We remark that adding the MILU(0) option to the existing ILU(0) implementation on GPUs is straightforward, which is left as our future work. The implementation of the GPU-based two-level multiplicative ILU method corresponding to Algorithm 2 is presented in Algorithm 5.

---

#### Algorithm 5 Multiplicative RAP-ILU on GPU

---

- 1: **procedure** RAP-ILU SETUP( $A$ ) ▷ Distributed CSR matrix
  - 2:   Compute local permutation  $p_i$
  - 3:   Permute  $A_i$  to  $A^{p_i}$  with  $p_i$
  - 4:   Call cuSPARSE to compute ILU(0)  $L_{A_i} U_{A_i} \approx A^{p_i}$
  - 5:   Compute MILU(0)  $\tilde{L}_{A_i} \tilde{U}_{A_i} \approx A^{p_i}$
  - 6:   Extract factors  $L_{B_i}$ ,  $U_{B_i}$ ,  $L_{S_i}$ ,  $U_{S_i}$ ,  $E_i U_{B_i}^{-1}$ , and  $L_{B_i}^{-1} F_i$
  - 7:   Setup triangular solve
  - 8:   **return**  $L_{A_i}$ ,  $U_{A_i}$ ,  $L_{B_i}$ ,  $U_{B_i}$ ,  $L_{S_i}$ ,  $U_{S_i}$ ,  $E_i U_{B_i}^{-1}$ , and  $L_{B_i}^{-1} F_i$
  - 9: **end procedure**
  - 10: **procedure** RAP-ILU SOLVE( $b$ ) ▷ Solve for  $x$  with right-hand-side  $b$
  - 11:   Call `thrust::gather` to permute  $b_i$  with  $p_i$
  - 12:   Call cuSPARSE to solve for  $L_{A_i} U_{A_i} x_i = b_i$
  - 13:   Call cuSPARSE to compute  $r = R(b - \hat{A}x)$
  - 14:   Apply GMRES to solve  $Sv = r$
  - 15:   Call cuSPARSE to compute  $\hat{x}_i = x_i + P_i r_i$
  - 16:   Call `thrust::scatter` to permute  $x_i$  with  $p_i$
  - 17:   **return**  $x$
  - 18: **end procedure**
-

## 4 Numerical Experiments

The numerical experiments for evaluating the proposed preconditioners were performed on the HPC clusters Ray and Lassen, both at the Lawrence Livermore National Laboratory. Each node of Ray has 4 NVIDIA P100 GPUs and 2 IBM POWER8 CPUs (dual-socket) with 10 cores. Each node on Lassen has 4 NVIDIA V100 GPUs and 2 IBM POWER9 CPUs (dual-socket) with 22 cores. The CUDA program was compiled using `nvcc` with the option `-gencode arch=compute_60,"code=sm_60"` for P100, and `compute_70, sm_70` for V100 respectively. The parallel ILU strategies presented in this paper have been implemented as part of a suite of parallel ILU smoothers and preconditioners, within the hypre [21] linear solver library. In what follows, we evaluate the performance of the various preconditioning techniques presented in this paper on elliptic PDE model problems. Here, we denote the block Jacobi ILU preconditioner by BJ-ILU, the additive two-level ILU preconditioner by SCHUR-ILU; the two-level multiplicative ILU preconditioner by RAP-ILU; and the two-level multiplicative MILU preconditioner by RAP-MILU.

### 4.1 Convergence Result

#### 4.1.1 ILU as preconditioners for GMRES

We begin our experiment by evaluating the performance of different ILU methods as the preconditioners for flexible GMRES (FGMRES). The reason for using FGMRES is that the preconditioner is not fixed, since GMRES is used to solve the global Schur complement system. Here, the GPU implementations of BJ-ILU, SCHUR-ILU, RAP-ILU, and RAP-MILU are evaluated. The restart dimension for FGMRES is set to 50 (FGMRES(50)), with a relative convergence tolerance of  $1.0e-8$ . We use the (M)ILU(0) variants of the factorization. Here, and in the remaining experiments, we use three steps of GMRES to solve the reduced system for the two-level methods.

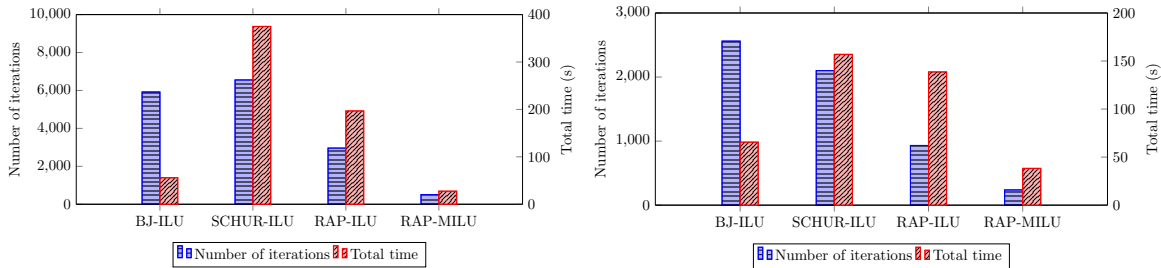
The model problem is a standard Laplacian problem defined as:

$$-\Delta u = f \quad \text{in } \Omega = [0, 1]^2 \text{ or } [0, 1]^3 \quad (34)$$

with the 5-pt stencil for 2D problem, and 7-pt stencil for 3D problem.

We run the first test using 16 nodes on Ray, giving a total of 64 MPI processes, with 4 MPI processes per node. For the 2D problem, we test a problem size of  $1024^2$ , and for the 3D problem, we test a size of  $512^3$ .

In the following tables, *its* is the number of outer iterations needed for the solver to converge, *p-t* is the time of the setup phase, and *s-t* is the time of the solve phase.



Preconditioner	#its	setup	solve
BJ-ILU(0)	5919	0.45	55.42
SCHUR-ILU(0)	6553	0.45	374.6
RAP-ILU(0)	2962	0.47	169.32
RAP-MILU(0)	514	0.51	27.12

a 2D Poisson problem of size  $1024^2$

Preconditioner	#its	setup	solve
BJ-ILU(0)	2561	1.23	64.38
SCHUR-ILU(0)	2100	1.4	155.56
RAP-ILU(0)	923	1.83	136.81
RAP-MILU(0)	238	3.91	34.38

b 3D Poisson problem of size  $512^3$

Figure 3: Iteration counts and timings of the block Jacobi preconditioner with ILU(0) and the two-level ILU(0)/MILU(0) preconditioners for 2-D/3-D Poisson problems along with FGMRES(50). The runs used 64 processes on 16 nodes.

Figure 3 highlights the results of this evaluation. The results indicate that the different methods are quite competitive. While BJ-ILU typically showed a slow rate of convergence, the time-to-solution was quite fast. On the other hand, SCHUR-ILU exhibits a slow rate of convergence that was proportional to its time-to-solution. The RAP strategies appear to be the better in both convergence rate and the time-to-solution for these test cases. In particular, we can clearly see the benefit of using the modified ILU approach to construct the interpolation

and restriction operators, thereby capturing important elliptic properties of the operator. Even though the setup costs for RAP-MILU is typically larger than the other options, the convergence rate was very fast, leading to the fastest total time.

In the next experiment, we perform a weak scaling study of those different strategies. The experiments are performed on up to 16 nodes on Ray with up to 4 MPI processes per node, to solve the system in (34). For the 2D problem, we keep the problem size on each subdomain fixed at  $256^2$ . We only show the result up to 32 processes, since BJ-ILU failed to converge within 20,000 steps. For the 3D problem, we keep the problem size in each subdomain as  $128^3$ .

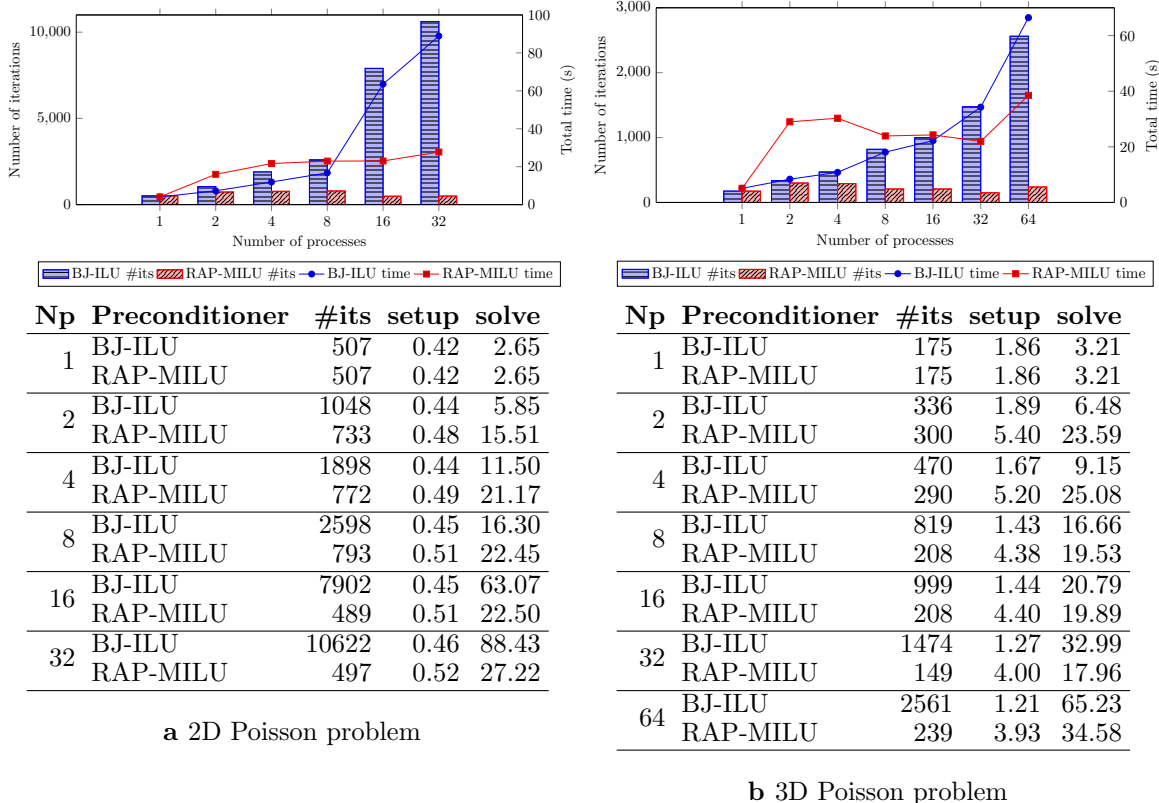


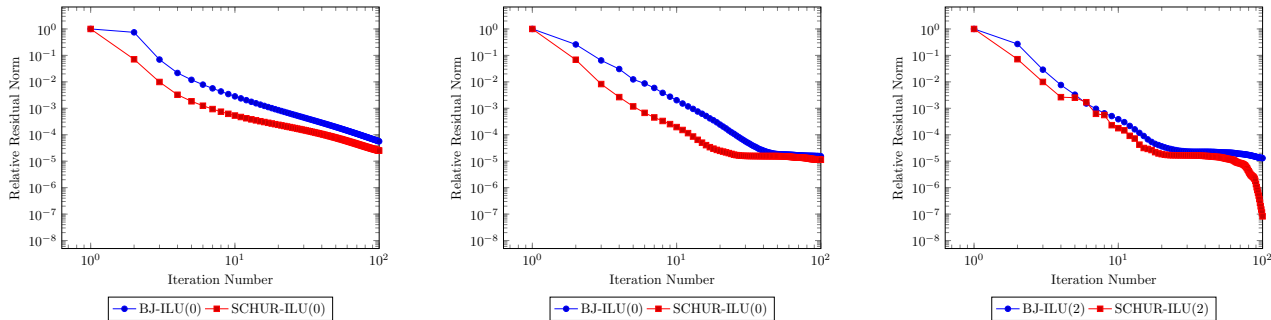
Figure 4: Weak scalability study of the block Jacobi with ILU(0) and the two-level ILU(0)/MILU(0) preconditioners for 2-D/3-D Poisson problems along with FGMRES(50) with up to 64 processes on 16 nodes of Ray. The problem size is  $256^2$  dofs per process for the 2D problem and  $128^3$  for the 3D problem.

According to the results in Figure 4, the RAP-MILU preconditioner has better weak scaling results. The number of iterations is more stable as the number of processes increases. In both cases, we observe an increase in the time to solution when the number of MPI processes is increased from 1 to 2. For the RAP-MILU preconditioner, this is primarily because RAP-MILU requires one classical ILU factorization and one modified ILU factorization, which increases the setup time. In addition, the solve time is also increased due to the additional MATVEC with  $S$ . For the BJ-ILU strategy, this is due to the lack of off-processor information in the factorization, which impacts its convergence properties. Thus, as we increase the number of MPI processes, we see a significant deterioration in the performance of BJ-ILU.

Next, we evaluate the performance of the ILU solvers as preconditioners for an application in multiphase flow in porous media. The problem is the solution of a linear system of equations arising from the simulation of a two-phase, two-component compositional flow model of  $\text{CO}_2$  injection. Details of the formulation and governing equations may be found in [9]. The resulting linear system captures the strong coupling between elliptic and hyperbolic dynamics associated with the unknowns. In addition, coupling between PDEs and algebraic constraint equations that govern well models at the injection sites leads to a complex linear system. These algebraic constraints also lead to equations with zero diagonal entries. This, coupled with the complex physical dynamics of the problem, leads to a linear system that is challenging to solve. Standard AMG is known to be ineffective for this problem, and strategies such as constrained pressure residual (CPR) [54, 55] and other block multilevel strategies have been proposed [56, 9] as efficient solution methods for this problem. CPR employs a two-stage process: a solve on a reduced system corresponding to the elliptic equations, followed by an approximate solve on the coupled global system. Both stages are essential for the convergence of CPR. The global system solve

is typically done with ILU (BJ-ILU), while the reduced system solve is performed with a scalable elliptic PDE solver like AMG. To mitigate the cost of solving the global system, typically only a few iterations of the global solver is applied.

In the results that follow, we demonstrate the performance of BJ-ILU and SCHUR-ILU as a standalone solver, and as a preconditioner for an FGMRES solver. The underlying linear system has a size of 614,400 and we fix the restart dimension for FGMRES to 100. We note that our implementation of the ILU factorization perturbs small entries on the diagonal to avoid breakdown of the factorization. Thus, the factorization is still successful even if the linear system matrix has zero diagonals. Figure 5 shows the convergence profiles for the first 100 iterations. The results indicate that the SCHUR-ILU strategy yields a better convergence rate than BJ-ILU, and thus would be effective as an approximate solver for the global system of the coupled problem. In the table in Figure 5, we present results on a strong scaling evaluation of the same problem with up to 64 MPI processes. Here, we set the convergence tolerance for FGMRES to  $10^{-5}$ , and use ILU(2) factorization. The results indicate that the SCHUR-ILU preconditioner is less sensitive to the change in the number of subdomains, and exhibits better convergence when the number of MPI processes is increased.



**a** ILU(0) without FGMRES.  $N_p=32$ . **b** ILU(0) with FGMRES(100).  $N_p=32$ . **c** ILU(2) with FGMRES(100).  $N_p=32$ .

$N_p$	SCHUR-ILU			BJ-ILU		
	#its	setup	solve	#its	setup	solve
1	89	8.75	23.49	89	8.75	23.49
2	80	4.64	10.59	82	4.33	10.47
4	57	2.36	4.13	92	2.10	5.86
8	68	1.19	2.50	96	1.05	3.09
16	74	0.65	1.55	97	0.52	1.61
32	85	0.33	0.98	129	0.24	1.04
64	94	0.17	0.64	222	0.11	0.88

**d** Strong scaling tests of BJ-ILU and SCHUR-ILU with ILU(2) as preconditioners for FGMRES(100). Up to 64 MPI processes are used.

Figure 5: Relative residual norm, iteration counts and timings of the BJ-ILU and the two-level additive SCHUR-ILU for solving the compositional flow problem.

#### 4.1.2 ILU as smoothers for AMG

In the following experiments in this section, we use BoomerAMG in hypre to evaluate the performance of our two-level ILU strategy as smoothers for AMG. The test problem is a Laplace problem modelled on a crooked pipe domain. We employ a finite element discretization using the MFEM package [2, 40]. A rendering of the resulting unstructured mesh, using GLVis [1], is shown in Figure 6. As shown in the figure, the mesh is inhomogeneous, which makes the problem challenging to solve.

In the first set of experiments, we compare the  $l_1$  Jacobi smoother with the two-level ILU smoothers. The two-level ILU methods are used as the smoother for the finest level of AMG. At the coarser levels, we use the  $l_1$  Jacobi smoother for all cases. The problem is discretized using a first order finite element discretization and the mesh is uniformly refined to get the desired problem size. We perform the tests on up to 32 MPI processes (without GPUs), using 2 nodes on the cluster Ray. For these tests, we evaluate the performance of both BJ-ILU and the two-level SCHUR-ILU using ILU(1). It is also worth mentioning that the standard BJ-ILU fails when

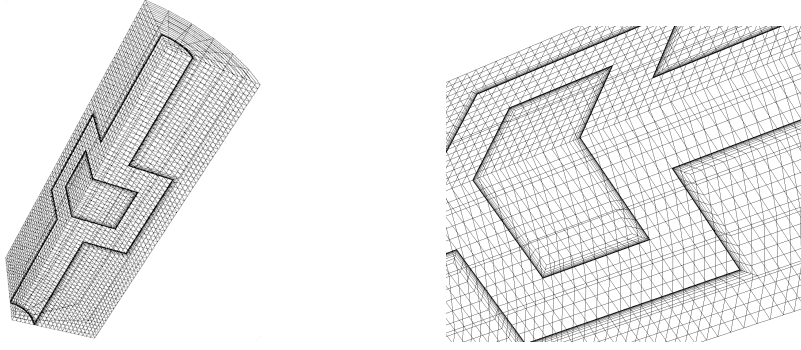


Figure 6: The mesh of the crooked pipe (left) and the zoom in of the center part (right).

the number of MPI processes is large. As a result, we use a variant of the BJ-ILU to improve the convergence rate. Instead of ignoring all off-diagonal block entries as in standard BJ methods, we use an  $l_1$ -BJ variant where we add the absolute values of the entries in off-diagonal blocks to the diagonal, that is for (3), we have

$$(A_i)_{k,k} = \sum_{i \neq j} \sum_l |(E_{i,j})_{k,l}|, \quad (35)$$

and then perform ILU factorization on  $A_i$ . The  $l_1$ -BJ approach can guarantee a convergent smoother for AMG when  $A$  is SPD and assuming the ILU factorization is accurate enough. For more discussions and analysis of  $l_1$  smoothers, see, e.g., [5].

We run our tests with two different coarsening algorithms: the parallel modified independent set (PMIS) coarsening, which generates the same coarse grid with different numbers of MPI processes; and the hybrid modified independent set (HMIS) coarsening that adds one extra step after PMIS to improve mesh quality, and for which however, the coarse grid can be very different for different number of MPI processes. According to the results in Table 1, the SCHUR-ILU smoother yields the best strong scaling results. For both coarsening algorithms, SCHUR-ILU is less sensitive to the change of the number of MPI processes.

Table 1: Iteration counts and timings of the  $l_1$ -block-Jacobi smoother with ILU(1) and the two-level additive ILU(1) smoother along with AMG for solving the crooked pipe problem. The number of unknowns is 966,609.

Np	$l_1$ -Jacobi			$l_1$ -BJ-ILU			SCHUR-ILU		
	#its	setup	solve	#its	setup	solve	#its	setup	solve
1	96	8.38	38.75	41	23.29	37.36	41	23.29	37.36
2	141	5.26	29.69	85	12.75	39.35	43	13.55	20.39
4	155	3.42	16.88	80	7.16	18.79	48	7.55	12.17
8	100	1.89	5.86	54	3.72	6.57	46	3.93	6.26
16	146	1.15	4.63	92	2.09	5.83	45	2.20	3.35
32	174	0.65	2.97	106	1.12	3.45	45	1.19	1.86

a AMG with HMIS coarsening

Np	$l_1$ -Jacobi			$l_1$ -BJ-ILU			SCHUR-ILU		
	#its	setup	solve	#its	setup	solve	#its	setup	solve
1	284	7.68	100.64	75	22.43	64.76	75	22.43	64.76
2	280	4.38	51.63	102	11.82	44.90	74	12.94	33.08
4	291	2.65	27.91	112	6.35	24.99	72	6.76	17.25
8	295	1.53	14.86	107	3.35	12.16	74	3.56	9.47
16	293	0.92	8.13	102	1.85	6.13	75	1.97	5.31
32	283	0.52	4.32	114	0.98	3.48	73	1.05	2.87

b AMG with PMIS coarsening

In the next set of experiments, we evaluate the performance of SCHUR-ILU with different mesh sizes and different orders for the finite element discretization. We use the same settings as the previous set of experiments,

except that the number of MPI processes is fixed at 32. As the results in Table 2 indicate, the SCHUR-ILU smoother typically works better than  $l_1$  Jacobi smoother. By replacing the smoother on the first level with SCHUR-ILU, we observe a reduction in the number of AMG cycles, which generally leads to a much faster solve phase. The SCHUR-ILU smoother requires some extra time in the setup phase, but the total time is in general smaller. Thus, it is easy to see that performance could be even better in a situation where multiple right-hand-sides are solved with the same linear system.

Table 2: Iteration counts and timings of the  $l_1$ -Jacobi smoother and the additive two-level ILU smoother with ILU(1) for solving the crooked pipe problem with different mesh sizes and different orders of finite elements. The runs used 32 MPI processes on 2 nodes.

Order	#Unknowns	Smoother	#its	setup	solve
1	126,805	$l_1$ -Jacobi	82	0.09	0.20
		SCHUR-ILU	48	0.15	0.30
1	966,609	$l_1$ -Jacobi	174	0.64	2.97
		SCHUR-ILU	45	1.19	1.86
1	7,544,257	$l_1$ -Jacobi	212	6.91	28.48
		SCHUR-ILU	58	11.37	18.09
2	126,805	$l_1$ -Jacobi	212	0.10	0.80
		SCHUR-ILU	30	0.30	0.45
2	966,609	$l_1$ -Jacobi	464	0.72	13.00
		SCHUR-ILU	47	2.28	4.58
3	414,472	$l_1$ -Jacobi	285	0.53	6.08
		SCHUR-ILU	27	2.45	2.58
3	3,209,173	$l_1$ -Jacobi	694	3.93	121.43
		SCHUR-ILU	34	18.57	19.50

These results demonstrate the usefulness of ILU methods as smoothers for AMG to solve challenging problems where simple smoothers lead to a slow convergence.

## 4.2 GPU Speedup

In the following experiments, we study the GPU speedup of our implementation by comparing the solve time of the same problem with and without GPU acceleration. The speedup of the triangular solves for the Nvidia cuSPARSE library has been studied in detail [42]. Here, we evaluate the GPU speedup of the two-level ILU methods as preconditioners for FGMRES, and the effect of the GPU version of the Schur complement strategy on the convergence rate.

We compare our GPU and CPU variants with all the available computing power on a single node. Since our algorithms are DD-based, the number of subdomains could influence the convergence. We use the same number of subdomains for the CPU runs, and the GPU runs. In addition, for the CPU tests, we enable OpenMP threading to use all the CPU cores on a single node. Thus, for the GPU tests on Ray, we use 4 MPI processes, each of which is bound to a GPU. For the corresponding CPU tests, we use 4 MPI processes, each with 5 OpenMP threads. The tests on Lassen have a similar setup, except that the number of OpenMP threads for each MPI process is 11 for the CPU runs. To bind MPI processors to physical cores, we use `mpibind` [32], which, on a single node, binds by socket first.

We report the performance of the CPU variant and GPU variant of BJ-ILU and two-level ILU methods and compute the speedup of all these options. We perform our evaluation on two sets of problems. In the first example, we consider a 3D discretized Laplacian problem on a  $128^3$  domain. We use ILU(0) and FGMRES(50) and report the speedup of the setup and the solve phase. Table 3 shows the results obtained on Ray (P100 GPU) and Lassen (V100 GPU). As the results indicate, we can have a total speedup of a factor of 3.38 for BJ-ILU, 2.52 for SCHUR-ILU, and 1.34 for RAP-MILU on Ray with P100 GPUs. With the V100 GPUs on Lassen, these numbers are 3.0, 1.2, and 1.74, respectively.

For the second example, we consider the compositional multiphase flow problem described earlier. The problem size is approximately 4.5 million. Recall that the problem formulation leads to the presence of zeros on the diagonal of the resulting coefficient matrix. This makes it infeasible to use the ILU(0) factorization in the cuSPARSE library. As a result, we perform the factorization on the CPU and transfer the resulting factors to the GPU for the solve phase. We use ILUT and ILU(1) factorizations for this evaluation. We note that the fill-factor of ILU(1) is roughly 1.8 and we choose a threshold such that the fill-factor for ILUT is also close to

Table 3: Iteration counts and timings (in seconds) of the CPU and the GPU implementations of the block-Jacobi preconditioner with ILU(0) and the two-level ILU(0) preconditioners along with FGMRES(50) for solving 3D Poisson problem of size  $128^3$  with 7pt Laplacians

Preconditioner	Device	#its	setup	solve	Preconditioner	Device	#its	setup	solve
BJ-ILU	CPU	229	0.17	8.35	BJ-ILU	CPU	229	0.15	6.07
	GPU	229	0.64	1.88		GPU	229	0.86	2.04
SCHUR-ILU	CPU	175	0.20	9.35	SCHUR-ILU	CPU	175	0.18	6.02
	GPU	175	0.65	3.14		GPU	175	0.7	5.28
RAP-MILU	CPU	154	0.20	9.11	RAP-MILU	CPU	154	0.27	17.96
	GPU	154	1.23	5.70		GPU	154	1.78	10.34

a P100 GPU (Ray)

b V100 GPU (Lassen)

1.8. We run 100 iterations of FGMRES(50) without restart and report the speedup the solve phase only. To allow for a fair comparison, we adjust the solver options for the two-level ILU preconditioner so that the relative residual after 100 iterations is similar between the CPU and GPU. Table 4 show the results obtained on Ray (P100 GPU) and Lassen (V100 GPU). The results indicate speedups of 2.62 for BJ-ILU with ILUT, 2.48 for BJ-ILU with ILU(1), 2.52 for Schur-ILU with ILUT, and 2.64 for Schur-ILU with ILU(1) on Ray with P100 GPUs. With the V100 GPUs on Lassen, these numbers are 1.78, 2.09, 2.12, and 2.14, respectively.

Notice that on Lassen, the GPU acceleration of the two-level ILU solve is much slower than that on Ray for the 3D discretized Laplacian problem. We found that this increase in solution time was caused by the performance of the sparse triangular solves associated with the local Schur complements. On the V100 GPUs, the sparse triangular solve operation is considerably slower than that on the P100 GPUs, and even slower than that on the CPU. We speculate that this is because the triangular factors are too small for the V100 GPUs to get a good speedup. We are currently investigating this issue further.

Table 4: Timings (in seconds) of the solve phase of the CPU and the GPU implementations of the block-Jacobi preconditioner with ILUT/ILU(1) and the two-level ILUT/ILU(1) preconditioners along with 100 steps of FGMRES for solving a compositional flow problem.

Preconditioner	Device	ILUT	ILU(1)	Preconditioner	Device	ILUT	ILU(1)
BJ-ILU	CPU	10.83	11.96	BJ-ILU	CPU	8.87	10.05
	GPU	4.13	4.83		GPU	4.98	4.80
SCHUR-ILU	CPU	17.03	15.67	SCHUR-ILU	CPU	13.04	14.35
	GPU	5.30	5.93		GPU	6.15	6.69

a P100 GPU (Ray)

b V100 GPU (Lassen)

### 4.3 Two-level ILU methods with ILU(k)

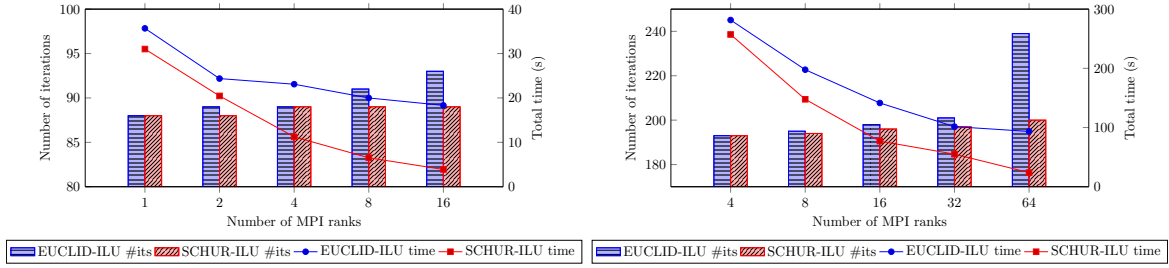
In the final set of experiments, we compare the performance of our proposed two-level ILU implementation to the two-level graph-based parallel ILU implementation in Euclid [26]. Euclid is also available through hypre, which makes is convenient to perform a fair evaluation of both strategies. The evaluation is performed on CPU only since Euclid is not GPU-enabled, and we focus on ILU(k), which is the parallel ILU variant supported by Euclid. The level of fill is chosen to be 2.

The model problem is a 3D convection diffusion problem defined as:

$$-\Delta u + b \cdot \nabla u = f \quad \text{in } [0, 1]^3 \quad (36)$$

and is discretized via finite differences with a 7-pt stencil. We perform strong scaling tests with MPI processes ranging from 1 to 16 on a problem of size  $128^3$ , and 4 to 64 on a problem of size  $256^3$ . The purpose of this experiment is to demonstrate the efficiency of the proposed ILU strategies compared to Euclid-ILU, implemented within the hypre linear solver library. To facilitate this comparison, we use the parallel ILU techniques as preconditioners for FGMRES(100) in order to obtain convergence for Euclid-ILU on these problems. The results are presented in Figure 7.





Np	Preconditioner	#its	setup	solve
1	EUCLID-ILU	88	8.42	27.25
	SCHUR-ILU	88	2.37	28.64
2	EUCLID-ILU	89	10.14	14.22
	SCHUR-ILU	88	1.15	19.30
4	EUCLID-ILU	89	15.59	7.50
	SCHUR-ILU	89	0.65	10.59
8	EUCLID-ILU	91	15.60	4.39
	SCHUR-ILU	89	0.33	6.19
16	EUCLID-ILU	93	15.72	2.60
	SCHUR-ILU	89	0.18	3.71

a 3D convection diffusion problem of size  $128^3$

Np	Preconditioner	#its	setup	solve
4	EUCLID-ILU	193	86.17	195.44
	SCHUR-ILU	193	5.18	252.02
8	EUCLID-ILU	195	83.86	113.83
	SCHUR-ILU	194	2.83	144.9
16	EUCLID-ILU	198	81.04	60.44
	SCHUR-ILU	196	1.41	75.64
32	EUCLID-ILU	201	77.35	24.15
	SCHUR-ILU	197	0.79	54.21
64	EUCLID-ILU	239	79.34	14.08
	SCHUR-ILU	200	0.38	23.50

b 3D convection diffusion problem of size  $256^3$

Figure 7: Strong scalability study of the EUCLID-ILU preconditioner and SCHUR-ILU preconditioner for 3D convection diffusion problems using FGMRES(100).

The results indicate that both parallel ILU strategies have similar convergence behavior, with Euclid exhibiting a slightly better solve time. However, the SCHUR-ILU strategy exhibits a superior strong scaling property in the setup costs, leading to a more efficient parallel ILU strategy overall.

Algebraic black-box solvers with multiple options, such as those presented in this paper have the benefit of being applicable to a wide class of problems. However, choosing the right options for a particular problem may require evaluating multiple options. Generally, it is appropriate to first consider cheaper strategies such as BJ-ILU(0) and RAP-MILU(0). Schur-ILU can be used if the convergence is not satisfactory. Increasing the level of fill for ILU(k) or switching to ILUT with a small drop tolerance should typically further improve the convergence. For most problems, we find that applying 3 iterations of GMRES, with ILU(0) as the preconditioner, on the coarse grid of the SCHUR-ILU method is enough to achieve good convergence. For more challenging problems, a more accurate ILU factorization and/ or a larger Krylov subspace dimension can be used to achieve better convergence. These tunable options enable users to control the cost vs. accuracy of the coarse grid solve, and thus, the performance of the preconditioner as a whole.

## 5 Conclusion

Motivated by the reliability of ILU preconditioners, we proposed a DD-based two-level parallel ILU strategy designed for distributed memory systems and with GPU support. We presented a detailed analysis of the two-level strategy, highlighting additive and multiplicative variants for constructing the Schur complement problem defining the global coupling between subdomains. We also demonstrate the benefit of using modified ILU to improve the spectral properties of the global Schur complement system, leading to a more accurate preconditioner. We adapt our algorithms to GPUs by leveraging existing optimized kernels for performing ILU(0) factorizations and triangular solves. Our implemented algorithms are readily available in hypre.

Numerical results demonstrate the effectiveness and scalability of the two-level parallel ILU preconditioner variants compared to the standard block Jacobi strategy. This is particularly evident when the size of the global Schur complement is large, corresponding to when a large number of processors are used. Nonetheless, for smaller number of subdomains or problems with weak inter-domain coupling, block Jacobi can be quite competitive. One good strategy, therefore, is to use block Jacobi whenever possible and switch to the more accurate two-level strategy when necessary. Our numerical results also indicate good GPU speedup. The amount of speedup typically depends on the matrix structure and problem size. For large problems with a good level structure in the triangular solve, GPU acceleration can yield significant performance gains compared to the CPU version.

Future work will consider implementing CUDA kernels that support permutation arrays for efficient ILU factorizations and triangular solves. We will also consider a multilevel ILU framework and its GPU version, to improve efficiency of the global Schur complement solve.

## References

- [1] GLVis: Opengl finite element visualization tool. [glvis.org](http://glvis.org).
- [2] R. Anderson, J. Andrej, A. Barker, J. Bramwell, J.-S. Camier, J. Cerveny V. Dobrev, Y. Dudouit, A. Fisher, Tz. Kolev, W. Pazner, M. Stowell, V. Tomov, I. Akkerman, J. Dahm, D. Medina, and S. Zampini. MFEM: A modular finite element library. *Computers & Mathematics with Applications*, 2020.
- [3] Hartwig Anzt, Stanimire Tomov, and Jack Dongarra. Accelerating the LOBPCG method on GPUs using a blocked sparse matrix vector product. In *Proceedings of the Symposium on High Performance Computing, HPC '15*, pages 75–82, San Diego, CA, USA, 2015. Society for Computer Simulation International.
- [4] Jared L. Aurentz, Vassilis Kalantzis, and Yousef Saad. Cucheb: A GPU implementation of the filtered Lanczos procedure. *Computer Physics Communications*, 220(Supplement C):332 – 340, 2017.
- [5] Allison H. Baker, Robert D. Falgout, Tzanio V. Kolev, and Ulrike Meier Yang. Multigrid smoothers for ultraparallel computing. *SIAM Journal on Scientific Computing*, 33(5):2864–2887, 2011.
- [6] Randolph E Bank and Christian Wagner. Multilevel ilu decomposition. *Numerische Mathematik*, 82(4):543–576, 1999.
- [7] EFF Botta and Fred W Wubs. Matrix renumbering ilu: An effective algebraic multilevel ilu preconditioner for sparse matrices. *SIAM Journal on Matrix Analysis and Applications*, 20(4):1007–1026, 1999.
- [8] Luc Buatois, Guillaume Caumon, and Bruno Lévy. Concurrent number cruncher: a GPU implementation of a general sparse linear solver. *International Journal of Parallel, Emergent and Distributed Systems*, 24(3):205–223, 2009.
- [9] Q. Bui, F. Hamon, N. Castelletto, D. Osei-Kuffuor, R. Settgast, and J. A. White. Multigrid reduction preconditioning framework for coupled processes in porous and fractured media. <https://arxiv.org/pdf/2101.11649.pdf>, 2021.
- [10] Xiao-Chuan Cai and Marcus Sarkis. A restricted additive schwarz preconditioner for general sparse linear systems. *Siam journal on scientific computing*, 21(2):792–797, 1999.
- [11] Luiz Mariano Carvalho, Luc Giraud, and Patrick Le Tallec. Algebraic two-level preconditioners for the schur complement method. *SIAM Journal on Scientific Computing*, 22(6):1987–2005, 2001.
- [12] Ü. V. Çatalyurek and C. Aykanat. Hypergraph-partitioning-based decomposition for parallel sparse-matrix vector multiplication. *IEEE Transactions on Parallel and Distributed Systems*, 10(7):673–693, 1999.
- [13] Juana Cerdán, José Marín, and José Mas. A two-level ilu preconditioner for electromagnetic applications. *Journal of Computational and Applied Mathematics*, 309:371–382, 2017.
- [14] Edmond Chow and Aftab Patel. Fine-grained parallel incomplete lu factorization. *SIAM journal on Scientific Computing*, 37(2):C169–C193, 2015.
- [15] Edmond Chow and Yousef Saad. Experimental study of ilu preconditioners for indefinite matrices. *Journal of Computational and Applied Mathematics*, 86(2):387–414, 1997.
- [16] M.A. Clark, R. Babich, K. Barros, R.C. Brower, and C. Rebbi. Solving lattice qcd systems of equations using mixed precision solvers on GPUs. *Computer Physics Communications*, 181(9):1517 – 1528, 2010.
- [17] Geoffrey Dillon, Vassilis Kalantzis, Yuanzhe Xi, and Yousef Saad. A hierarchical low rank schur complement preconditioner for indefinite linear systems. *SIAM Journal on Scientific Computing*, 40(4):A2234–A2252, 2018.
- [18] A. Dziekonski, M. Rewienski, P. Sypek, A. Lamecki, and M. Mrozowski. GPU-accelerated LOBPCG method with inexact null-space filtering for solving generalized eigenvalue problems in computational electromagnetics analysis with higher-order fem. *Communications in Computational Physics*, 22(4):997–1014, 2017.
- [19] Yogi A Erlangga, Cornelis W Oosterlee, and Cornelis Vuik. A novel multigrid based preconditioner for heterogeneous helmholtz problems. *SIAM Journal on Scientific Computing*, 27(4):1471–1492, 2006.
- [20] Yogi A Erlangga, Cornelis Vuik, and Cornelis W Oosterlee. Comparison of multigrid and incomplete lu shifted-laplace preconditioners for the inhomogeneous helmholtz equation. *Applied numerical mathematics*, 56(5):648–666, 2006.
- [21] Robert D Falgout and Ulrike Meier Yang. hypre: A library of high performance preconditioners. In *International Conference on Computational Science*, pages 632–641. Springer, 2002.

- [22] Rajesh Gandham, Kenneth Esler, and Yongpeng Zhang. A GPU accelerated aggregation algebraic multigrid method. *Computers & Mathematics with Applications*, 68(10):1151 – 1160, 2014.
- [23] Simon Gawlok, Philipp Gerstner, Saskia Haupt, Vincent Heuveline, Jonas Kratzke, Philipp Lösel, Katrin Mang, Mareike Schmidtobreck, Nicolai Schoch, Nils Schween, Jonathan Schwegler, Chen Song, and Martin Wlotzka. Hiflow3 – technical report on release 2.0. *Preprint Series of the Engineering Mathematics and Computing Lab (EMCL)*, 0(06), 2017.
- [24] Norman E Gibbs, William G Poole, Jr, and Paul K Stockmeyer. An algorithm for reducing the bandwidth and profile of a sparse matrix. *SIAM Journal on Numerical Analysis*, 13(2):236–250, 1976.
- [25] B. Hendrickson and R. Leland. *The Chaco User’s Guide Version 2*. Sandia National Laboratories, Albuquerque NM, 1994.
- [26] David Hysom and Alex Pothén. Efficient parallel computation of ilu (k) preconditioners. In *Proceedings of the 1999 ACM/IEEE conference on Supercomputing*, pages 29–es, 1999.
- [27] Joseph E. Pasciak James H. Bramble and Jinchao Xu. Parallel multilevel preconditioners\* james h. bramblet joseph e. pasciak. *Mathematics of Computation*, 55:1–22, 1990.
- [28] G. Karypis and V. Kumar. A fast and high quality multilevel scheme for partitioning irregular graphs. *SIAM Journal on Scientific Computing*, 20(1):359–392, 1998.
- [29] George Karypis and Vipin Kumar. Parallel threshold-based ilu factorization. In *SC’97: Proceedings of the 1997 ACM/IEEE Conference on Supercomputing*, pages 28–28. IEEE, 1997.
- [30] T. G. Kolda. Partitioning sparse rectangular matrices for parallel processing. *Lecture Notes in Computer Science*, 1457:68–79, 1998.
- [31] PARALUTION Labs. Paralution v1.1.0, 2016. <http://www.paralution.com/>.
- [32] Edgar A. León. Mpibind: A memory-centric affinity algorithm for hybrid applications. In *Proceedings of the International Symposium on Memory Systems, MEMSYS ’17*, page 262–264, New York, NY, USA, 2017. Association for Computing Machinery.
- [33] R. Li and Y. Saad. GPU-accelerated preconditioned iterative linear solvers. *The Journal of Supercomputing*, 63:443–466, 2013.
- [34] R. Li, Y. Xi, L. Erlandson, and Y. Saad. The eigenvalues slicing library (EVSL): Algorithms, implementation, and software. *SIAM Journal on Scientific Computing*, 41(4):C393–C415, 2019.
- [35] Zhongze Li, Yousef Saad, and Masha Sosonkina. parms: a parallel version of the algebraic recursive multilevel solver. *Numerical linear algebra with applications*, 10(5-6):485–509, 2003.
- [36] Xiao Liu, Yuanzhe Xi, Yousef Saad, and Maarten V de Hoop. Solving the 3d high-frequency helmholtz equation using contour integration and polynomial preconditioning. *arXiv preprint arXiv:1811.12378*, 2018.
- [37] Li Luo, Yubo Zhao, and Xiao-Chuan Cai. A hybrid implementation of two-level domain decomposition algorithm for solving elliptic equation on cpu/gpus. In *2012 13th International Conference on Parallel and Distributed Computing, Applications and Technologies*, pages 474–477. IEEE, 2012.
- [38] Mardochée Magolu Monga Made, Robert Beauwens, and Guy Warzée. Preconditioning of discrete helmholtz operators perturbed by a diagonal complex matrix. *Communications in numerical methods in engineering*, 16(11):801–817, 2000.
- [39] Thomas A Manteuffel. An incomplete factorization technique for positive definite linear systems. *Mathematics of computation*, 34(150):473–497, 1980.
- [40] MFEM: Modular finite element methods [Software]. [mfem.org](http://mfem.org).
- [41] M. Naumov, M. Arsaev, P. Castonguay, J. Cohen, J. Demouth, J. Eaton, S. Layton, N. Markovskiy, I. Reguly, N. Sakharnykh, V. Sellappan, and R. Strzodka. AmgX: A library for GPU accelerated algebraic multigrid and preconditioned iterative methods. *SIAM Journal on Scientific Computing*, 37(5):S602–S626, 2015.
- [42] Maxim Naumov. Parallel solution of sparse triangular linear systems in the preconditioned iterative methods on the gpu. *NVIDIA Corp., Westford, MA, USA, Tech. Rep. NVR-2011*, 1, 2011.
- [43] Maxim Naumov, Patrice Castonguay, and Jonathan Cohen. Parallel graph coloring with applications to the incomplete-lu factorization on the gpu. *Nvidia White Paper*, 2015.
- [44] Italo Cristiano L Nievinski, Michael Souza, Paulo Goldfeld, Douglas Adriano Augusto, José Roberto P Rodrigues, and Luiz Mariano Carvalho. Parallel implementation of a two-level algebraic ilu (k)-based domain decomposition preconditioner. *TEMA (São Carlos)*, 19(1):59–77, 2018.

- [45] F. Pellegrini. *Scotch and libScotch 5.1 User's Guide*. INRIA Bordeaux Sud-Ouest, IPB & LaBRI, UMR CNRS 5800, 2010.
- [46] A. Pothen, H. D. Simon, and K. P. Liou. Partitioning sparse matrices with eigenvectors of graphs. *SIAM Journal on Matrix Analysis and Applications*, 11:430–452, 1990.
- [47] Steven C. Rennich, Darko Stosic, and Timothy A. Davis. Accelerating sparse Cholesky factorization on GPUs. *Parallel Computing*, 59(Supplement C):140 – 150, 2016. Theory and Practice of Irregular Applications.
- [48] C. Richter, S. Schöps, and M. Clemens. GPU acceleration of algebraic multigrid preconditioners for discrete elliptic field problems. *IEEE Transactions on Magnetics*, 50(2):461–464, Feb 2014.
- [49] Karl Rupp, Philippe Tillet, Florian Rudolf, Josef Weinbub, Andreas Morhammer, Tibor Grasser, Ansgar Jüngel, and Siegfried Selberherr. ViennaCL—linear algebra library for multi- and many-core architectures. *SIAM Journal on Scientific Computing*, 38(5):S412–S439, 2016.
- [50] Yousef Saad and Jun Zhang. Bilutm: a domain-based multilevel block ilut preconditioner for general sparse matrices. *SIAM Journal on Matrix Analysis and Applications*, 21(1):279–299, 1999.
- [51] Piyush Sao, Richard Vuduc, and Xiaoye Sherry Li. A distributed cpu-gpu sparse direct solver. In *European Conference on Parallel Processing*, pages 487–498. Springer, 2014.
- [52] Martin B van Gijzen, Yogi A Erlangga, and Cornelis Vuik. Spectral analysis of the discrete helmholtz operator preconditioned with a shifted laplacian. *SIAM Journal on Scientific Computing*, 29(5):1942–1958, 2007.
- [53] Panayot S Vassilevski and Ulrike Meier Yang. Reducing communication in algebraic multigrid using additive variants. *Numerical Linear Algebra with Applications*, 21(2):275–296, 2014.
- [54] J. R. Wallis. Incomplete gaussian elimination as a preconditioning for generalized conjugate gradient acceleration. In *SPE Reservoir Simulation Symposium*. Society of Petroleum Engineers, 1983.
- [55] J. R. Wallis, R. P. Kendall, and L. E. Little. Constrained residual acceleration of conjugate residual methods. In *SPE Reservoir Simulation Symposium*. Society of Petroleum Engineers (SPE), 1985.
- [56] L. Wang, D. Osei-Kuffuor, R. D. Falgout, I. D. Mishev, and J. Li. Multigrid reduction for coupled flow problems with application to reservoir simulation. In *SPE Reservoir Simulation Conference*. Society of Petroleum Engineers (SPE), SPE-182723-MS, 2017.
- [57] Mingliang Wang, Hector Klie, Manish Parashar, and Hari Sudan. Solving sparse linear systems on nvidia tesla gpus. In *International Conference on Computational Science*, pages 864–873. Springer, 2009.
- [58] Yuanzhe Xi and Yousef Saad. A rational function preconditioner for indefinite sparse linear systems. *SIAM Journal on Scientific Computing*, 39(3):A1145–A1167, 2017.